



Aero-Engines AI—A Machine-Learning App for Aircraft Engine Concepts Assessment

Michael T. Tong
Glenn Research Center, Cleveland, Ohio

NASA STI Program . . . in Profile

Since its founding, NASA has been dedicated to the advancement of aeronautics and space science. The NASA Scientific and Technical Information (STI) Program plays a key part in helping NASA maintain this important role.

The NASA STI Program operates under the auspices of the Agency Chief Information Officer. It collects, organizes, provides for archiving, and disseminates NASA's STI. The NASA STI Program provides access to the NASA Technical Report Server—Registered (NTRS Reg) and NASA Technical Report Server—Public (NTRS) thus providing one of the largest collections of aeronautical and space science STI in the world. Results are published in both non-NASA channels and by NASA in the NASA STI Report Series, which includes the following report types:

- TECHNICAL PUBLICATION. Reports of completed research or a major significant phase of research that present the results of NASA programs and include extensive data or theoretical analysis. Includes compilations of significant scientific and technical data and information deemed to be of continuing reference value. NASA counter-part of peer-reviewed formal professional papers, but has less stringent limitations on manuscript length and extent of graphic presentations.
- TECHNICAL MEMORANDUM. Scientific and technical findings that are preliminary or of specialized interest, e.g., “quick-release” reports, working papers, and bibliographies that contain minimal annotation. Does not contain extensive analysis.
- CONTRACTOR REPORT. Scientific and technical findings by NASA-sponsored contractors and grantees.
- CONFERENCE PUBLICATION. Collected papers from scientific and technical conferences, symposia, seminars, or other meetings sponsored or co-sponsored by NASA.
- SPECIAL PUBLICATION. Scientific, technical, or historical information from NASA programs, projects, and missions, often concerned with subjects having substantial public interest.
- TECHNICAL TRANSLATION. English-language translations of foreign scientific and technical material pertinent to NASA's mission.

For more information about the NASA STI program, see the following:

- Access the NASA STI program home page at <http://www.sti.nasa.gov>
- E-mail your question to help@sti.nasa.gov
- Fax your question to the NASA STI Information Desk at 757-864-6500
- Telephone the NASA STI Information Desk at 757-864-9658
- Write to:
NASA STI Program
Mail Stop 148
NASA Langley Research Center
Hampton, VA 23681-2199



Aero-Engines AI—A Machine-Learning App for Aircraft Engine Concepts Assessment

Michael T. Tong
Glenn Research Center, Cleveland, Ohio

Prepared for the
ASME Turbo Expo 2023: Turbine Technical Conference and Exposition
sponsored by American Society of Mechanical Engineers
Boston, Massachusetts, June 26–30, 2023

National Aeronautics and
Space Administration

Glenn Research Center
Cleveland, Ohio 44135

Acknowledgments

The work presented in this paper was supported by the NASA Advanced Air Transport Technology Project of the Advanced Air Vehicles Program.

This report contains preliminary findings,
subject to revision as analysis proceeds.

This work was sponsored by the Advanced Air Vehicle Program
at the NASA Glenn Research Center

Trade names and trademarks are used in this report for identification
only. Their usage does not constitute an official endorsement,
either expressed or implied, by the National Aeronautics and
Space Administration.

Level of Review: This material has been technically reviewed by technical management.

Aero-Engines AI—A Machine-Learning App for Aircraft Engine Concepts Assessment

Michael T. Tong
National Aeronautics and Space Administration
Glenn Research Center
Cleveland, Ohio 44135

Abstract

Effective deployment of machine-learning (ML) models could drive a high level of efficiency in aircraft engine conceptual design. *Aero-Engines AI* is a user-friendly app that has been created to deploy trained machine-learning (ML) models to assess aircraft engine concepts. It was created using *tkinter*, a GUI (graphical user interface) module that is built into the standard Python library. Employing *tkinter* greatly facilitates the sharing of ML application as an executable file which can be run on Windows machines (without the need to have Python or any library installed). The app gets user input for a turbofan design, preprocesses the input data, and deploys trained ML models to predict turbofan thrust specific fuel consumption (TSFC), engine weight, core size, and turbomachinery stage-counts. The ML predictive models were built by employing supervised deep-learning and K-nearest neighbor regression algorithms to study patterns in an existing open-source database of production and research turbofan engines. They were trained, cross-validated, and tested in Keras, an open-source neural networks API (application programming interface) written in Python, with TensorFlow (Google open-source artificial intelligence library) serving as the backend engine. The smooth deployment of these ML models using the app shows that *Aero-Engines AI* is an easy-to-use and a time-saving tool for aircraft engine design-space exploration during the conceptual design stage. Current version of the app focuses on the performance prediction of conventional turbofans. However, the scope of the app can easily be easily expanded to include other engine types (such as turboshaft and hybrid-electric systems) after their ML models are developed. Overall, the use of a machine-learning app for aircraft engine concept assessment represents a promising area of development in aircraft engine conceptual design.

Introduction

More and more organizations are adopting a data-informed approach to decision-making. With the vast amounts of data collected and tracked in recent times, machine-learning (ML) applications are gaining popularity across multiple industries.

The aircraft engine industry has amassed and stored significant quantities of data over the years. These big data sets, sourced from multiple origins such as the database of currently manufactured engines, ongoing development projects, previously completed development projects, and unmanufactured designs, hold tremendous potential as a knowledge asset for future engine projects.

Designing an aircraft engine is a complex, interdisciplinary process that requires significant time and effort. Engine designers encounter a formidable challenge during the conceptual design phase - how to rapidly evaluate the performance of a specific engine design given the aircraft's mission requirements and various design parameters. The number of potential engine configurations could be vast, requiring designers to rely on system analysis and simulation to estimate performance. Consequently, designers must conduct a comprehensive propulsion system study for each possible configuration, which can be time-consuming, particularly when dealing with a large design space.

By leveraging the power of machine learning (ML) algorithms to learn from the existing engine data sets, it is possible to develop ML models that can quickly and accurately assess new aircraft engine concepts, providing valuable insights and reducing the time and resources required for the engine concept assessment process. A ML model can identify patterns and trends that may not be immediately apparent to human analysts, leading to more informed decision-making and ultimately resulting in the development of better aircraft engine concepts. The ability to assess new engine concepts quickly and accurately can be a competitive advantage in aircraft engine development.

Previously, the author focused on training/developing the ML models that allow for quick estimation of engine TSFC, system weight, and core size during the conceptual design phase. The development process and methodology for these models are described in References 1 to 3. Additional ML models were developed for the turbomachinery stage count prediction since then, using the same methodology. This paper zeros in on the deployment of these trained ML models to assess aircraft engine concepts, via an app. The development process of the app, *Aero-Engines AI*, is described in this paper.

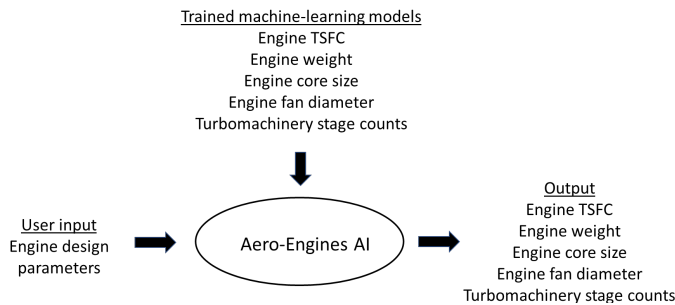


Figure 1.—Structure of *Aero-Engines AI* app.

While the development of ML models is essential for their applications, the models would only be of value if they are actively deployed in a production environment where they can be used to solve practical problems. Thus, effective ML model deployment is just as important as ML model development. ML model deployment involves integrating trained ML models, developed in a R&D environment, into a production environment. It is a critical step that must be done so an organization can use the models to solve problems. Seamless deployment of trained ML models into production is essential for putting the models to practical use.

Aero-Engines AI, a Windows app, has been created to deploy the trained ML models for aircraft engine concepts assessment. It was created using *tkinter*, a GUI module that is built into the standard Python library. Employing *tkinter* greatly facilitates the sharing of ML application as an executable file which can be run on Windows machines (without the need to have Python or any library installed). MS Windows platform was chosen for the deployment to reduce complexity and for ease of access. The structure of the app is shown in Figure 1.

The app is user-friendly. It is simple to learn, easy to navigate, and its use is intuitive enough that it does not require an instruction manual. The development process of *Aero-Engines AI* consists of five steps:

1. Engine data collection, augmentation, and preparation
2. ML models training
3. ML models testing and evaluation
4. App design for ML models deployment
5. Monitoring and updating

Engine Data Collection, Augmentation, and Preparation

Engine Data Collection

Current version of the app has only turbofan assessment capability (will be expanded to include other engine types such as turboshaft, hybrid-turbofan, etc., in the future versions). The basic engine architecture is an axial-compressor turbofan. The

engine database consists of 145 manufactured (commercial) engines (Refs. 4 to 10) and 39 engines that were studied previously in various NASA aeronautics projects. These commercial engines capture over half-a-century of engine technology improvements and lessons-learned, which would minimize the prediction uncertainties of the ML models. The NASA engine data were the system-study results for various NASA aeronautics projects (Refs. 11 to 16). The engine database is shown in Appendix A.

Data Augmentation

Data augmentation is an important technique that is commonly used in ML to improve the performance and generalizability of a training model. The process entails creating additional data points from the existing training data by applying various transformations and modifications to the data. Data augmentation increases the diversity and quantity of training data, improving the model's performance for its task, and making it more adaptable to changes in the data. For this study, the data augmentation was performed by scaling up the current engines by 10 percent. For example, the sea-level static (SLS) engine thrust and weight were increased by 10 percent, while keeping the other operating parameters such as bypass ratio (BPR), overall pressure ratio (OPR), Mach No., altitude, and TSFC unchanged, as shown below:

BPR	OPR	SLS Thrust (lbs)	Mach	Alt. (ft)	TSFC (lb/hr/lb)	Weight (lbs)
8.44	38.37	79377	0.85	35000	.5526	18949
8.44	38.37	87315	0.85	35000	.5526	20844

With the data augmentation, the size of the database becomes:

<u>Turbofan type</u>	<u>No. of engines</u>
2-spool direct-drive	273
2-spool geared	89
3-spool direct-drive	50

Dataset Preparation

The next step was to prepare the data that would be used to train the ML models. It involved cleaning and preprocessing the data to remove errors or inconsistencies and organizing the data into a format that could be used for the training. The engine dataset was normalized and shuffled randomly (using pseudo-random number generator) and divided into two datasets: the training set and the testing set. The training set was used to train, cross-validate, and build predictive models. The testing set consisted of the remaining engines that were unseen by the training models and was retained for the final evaluation of the predictive analytics. The dataset preparation is described in detail in References 1 to 3.

ML Models Training

Once the data was ready, the next step was to select the appropriate algorithms that would be used to train the ML models. This can involve choosing from a variety of machine learning algorithms and tuning the parameters and hyperparameters of the models to optimize their performance on the specific problem or task.

As reported in References 1 to 3, the ML models for TSFC, engine weight, and core size predictions were constructed using supervised deep-learning and K-nearest neighbor algorithms (Ref. 17), which analyzed patterns in an open-source database of research and production turbofan engines. Additional ML models were developed since then for the turbomachinery stage count prediction, using K-nearest neighbor regression algorithm. These models were trained, cross-validated, and tested using Keras, an open-source neural networks API written in Python, with TensorFlow as the backend engine. These models were trained and deployed in Keras (Ref. 18), an open-source neural networks API written in Python, with TensorFlow (Ref. 19) serving as the backend engine. Keras provided the building blocks for developing the deep-learning models, and TensorFlow handled the tensor computations and manipulations.

Depending on the ML model, either *L2* or *Dropout* regularization technique (where neuron outputs are dropped out randomly) (Refs. 20 and 21) was applied to prevent the DNN from overfitting the training data. A grid-search routine was used to determine the regularization parameter, dropout rate, number of epochs, batch size, and the number of ‘neurons’ in the hidden layers that give the lowest training error. The Adam optimization algorithm (Ref. 22) was used to update the network weights during each epoch.

Totally, nine ML models were trained for engine *TSFC*, *weight*, *core size* (last stage HPC blade height), fan diameter, and *turbomachinery stage count* predictions, respectively. The training and cross validation of these ML models are described in detail in References 1 to 3.

ML Models Testing

After the ML models were trained, the next step was to test and evaluate their performances. The trained ML models were evaluated using a separate set of data, the testing dataset (that was unseen by the training models). The testing procedures of these ML models are described in detail in References 1 to 3. The results showed that these ML models are an effective tool for predicting engine TSFC, engine weight, core size, and turbomachinery stage counts. Their performances were determined, in terms of the means and standard deviations, as shown in Table I.

TABLE I.—ML MODELS PERFORMANCE

ML model	Mean accuracy, percent	Uncertainty 95% confidence interval (2 standard deviations)
TSFC	98	4%
Weight	95	5%
Core size	98	4%
Fan diameter	98	5%
LPC stage count	98	14% (or 1 stage) ^a
HPC stage count	98	8% (or 1 stage) ^a
HPT stage count	96	39% (or 1 stage) ^a
LPT stage count	98	18% (or 1 stage) ^a
IPT stage count	90	44% (or 1 stage) ^a

^aBased on the current database. 1-stage fan is assumed for all the engines.

APP Design for ML Models Deployment

After the ML models were developed, trained, and tested, they were integrated into the user-friendly app, *Aero-Engines AI*, that allows for the easy and intuitive assessment of engine concepts. *Aero-Engines AI* is a Windows app that deploys trained ML models to assess aircraft engine concepts. The app was created using *tkinter* (Ref. 23), a GUI (graphical user interface) module that is built into the standard Python library. And *pyinstaller* (Ref. 24), a Python package, was used to convert the python scripts into an executable file that can be run on Windows machines. The conversion greatly facilitates the sharing of ML applications with other Windows users (who do not need to have Python, or any library installed in their computers).

The app design aimed to provide a user-friendly experience with a simple point-and-click feature. The input page consists of three elements:

1. a drop-down menu to select options
2. data entry fields
3. a ‘PREDICT’ button to run the app

These three elements are shown in Figure 2.

The drop-down menu allows users to select different options for engine architectures, configurations, and timeframe. When a user selects a tab, the drop-down menu will display the options that are associated with that tab. Based on the user's selection, the app would use the trained ML models to analyze relevant data and make predictions on engine performance, in terms of engine TSFC, weight, core size, and turbomachinery stage counts.

The drop-down menu consists of the following tabs:

Engine type—current version of the app only has the conventional turbofans option. Turbohaft and hybrid-electric turbofan are being considered for the future app versions. The engine-type tab is shown in Figure 3.

Drive system—offers two options: direct-drive or geared. This tab is shown in Figure 4.

Engine configuration—offers two options: 2-spool or 3-spool design. This tab is shown in Figure 5.

Engine timeframe—engine certified year. Users can pick a calendar year or NASA timeframe (N+1, N+2, etc.). This tab is shown in Figure 6.

Single engine or Multiple engine designs—offers two options: single engine design or multiple-engine designs analyses. This tab is shown in Figure 7. If “multiple engine designs” is selected, the user inputs for bypass ratio, overall pressure ratio, and engine thrust would be in ranges, as shown in Figure 8.

The data entry fields are provided for the users to input the engine design parameters. The default entries for the Mach number and cruise altitude are provided (0.8 and 35000 ft, respectively), as shown in Figure 2. The users can override these numbers.

App execution—to run the app, one simply clicks the ‘PREDICT’ button.

Input changes—users can return to the input page and modify the inputs by clicking the ‘BACK’ button on the output page. This button is shown in Figure 9.

Example Problems

- Single engine design:
 - input parameters are shown in Figure 7
 - outputs are shown in Figure 9
- Multiple engine designs:
 - input parameters are shown in Figure 8
 - output spreadsheet is shown in Figure 10

Monitoring and Updating

Monitoring and updates are important aspects of ML app development, as they help ensure that the app continues to perform well and provide accurate predictions or recommendations over time. To ensure optimal performance of the current ML models, it’s crucial to keep track of the changing engine data and its effect on their overall functionality. While the commercial engine data in the current database remain static, the NASA engine data are obtained through research on aeronautics studies for three generations of aircraft - near, mid, and far term. Each generation has associated goals for reductions in noise, emissions, fuel burn, and field length relative to present-day aircrafts. These aircraft generations are labeled as 'N+1', 'N+2', and 'N+3', respectively. The research for 'N+2' and 'N+3' is aimed at enabling new vehicle configurations that meet NASA’s ambitious technology objectives. As the NASA engine data could be revised over time, the ML models must be updated periodically to consider the impact of such updates.

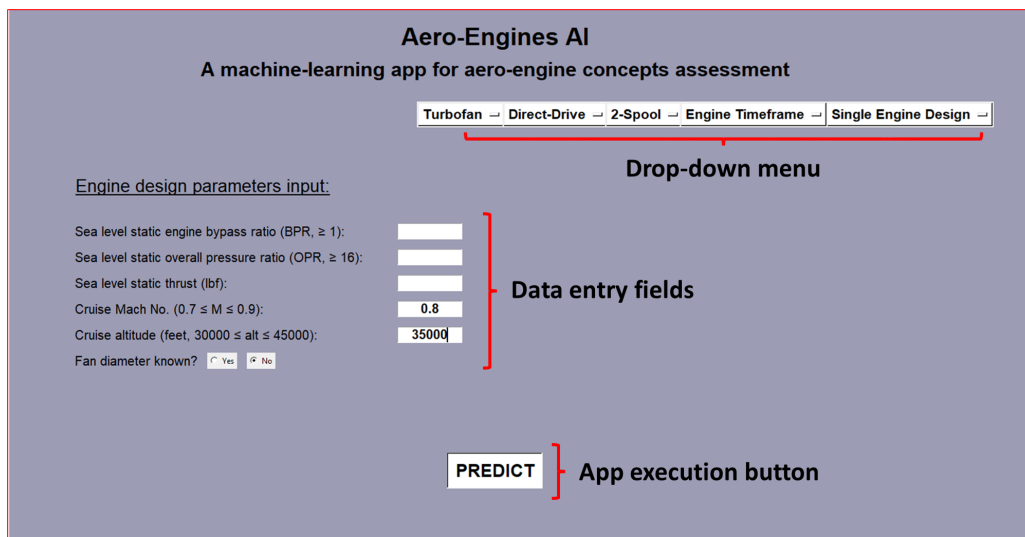


Figure 2.—User input page for single-engine design.

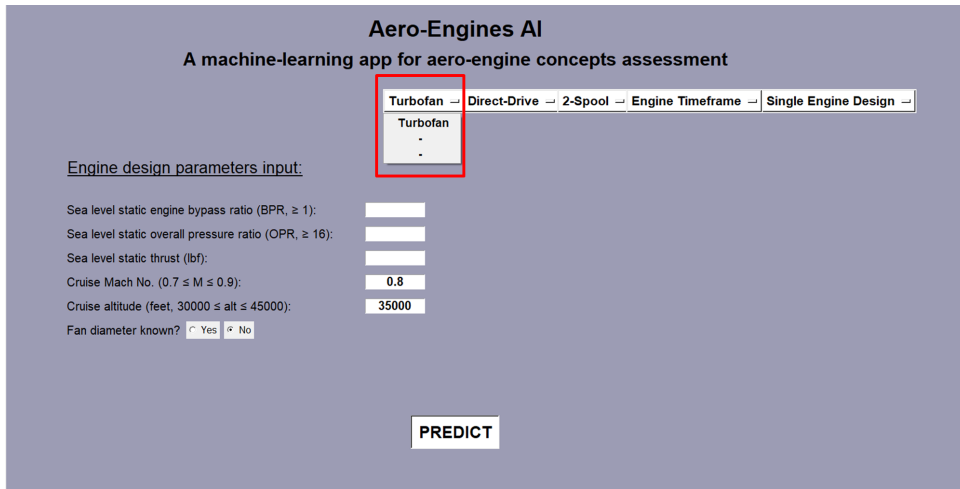


Figure 3.—Engine type option.

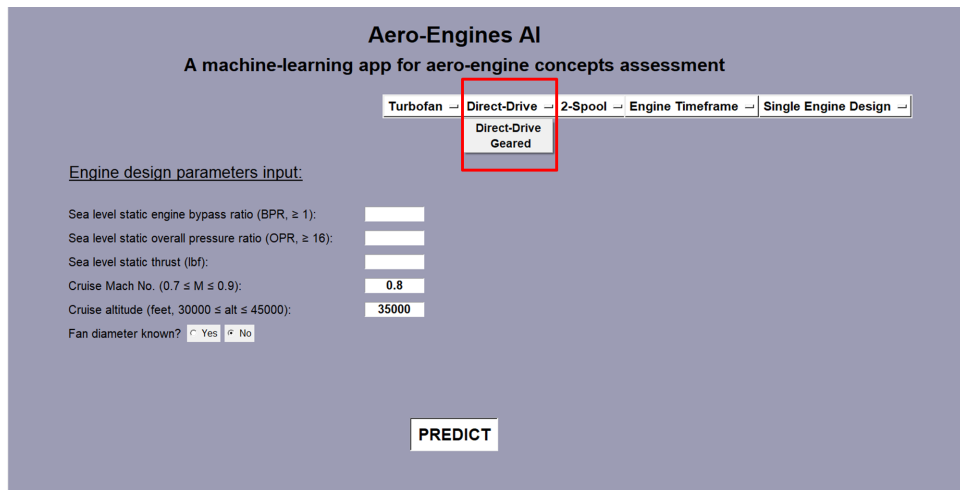


Figure 4.—Direct-drive or geared turbofan option.

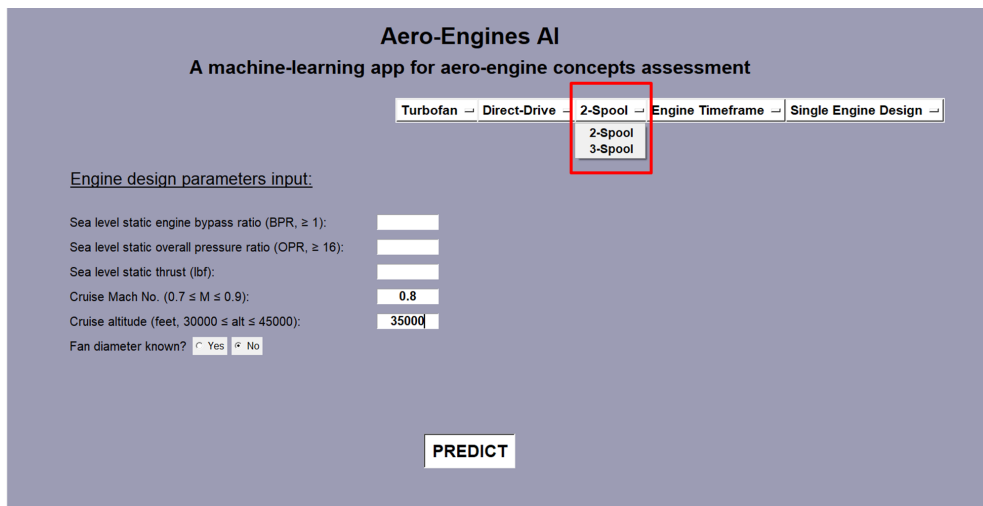


Figure 5.—Engine configuration options.

Aero-Engines AI
A machine-learning app for aero-engine concepts assessment

Turbofan Direct-Drive 2-Spool Engine Timeframe Single Engine Design

Engine design parameters input:

Sea level static engine bypass ratio (BPR, ≥ 1):

Sea level static overall pressure ratio (OPR, ≥ 16):

Sea level static thrust (lbf):

Cruise Mach No. ($0.7 \leq M \leq 0.9$):

Cruise altitude (feet, $30000 \leq \text{alt} \leq 45000$):

Fan diameter known? Yes No

PREDICT

Engine Timeframe

Year 2020

Year 2025

Year 2030

Year 2035

Year 2040

Year 2045

Year 2050

NASA N+1

NASA N+2

NASA N+3

NASA N+4

Figure 6.—Engine timeframe option.

Aero-Engines AI
A machine-learning app for aero-engine concepts assessment

Turbofan Direct-Drive 2-Spool Year 2020 Single Engine Design

Engine design parameters input:

Sea level static engine bypass ratio (BPR, ≥ 1):

Sea level static overall pressure ratio (OPR, ≥ 16):

Sea level static thrust (lbf):

Cruise Mach No. ($0.7 \leq M \leq 0.9$):

Cruise altitude (feet, $30000 \leq \text{alt} \leq 45000$):

Fan diameter known? Yes No

PREDICT

Single Engine Design

Multiple Engine Designs

Figure 7.—Single-engine or multiple-engine design option.

Aero-Engines AI
A machine-learning app for aero-engine concepts assessment

Turbofan Geared 2-Spool Year 2035 Multiple Engine Designs

Engine design parameters input:

Sea level static engine bypass ratio range (BPR): (min, ≥ 1) (max, <36) (max. no. of step)

Sea level static overall pressure ratio range (OPR): (min, ≥ 16) (max, <55) (max. no. of step)

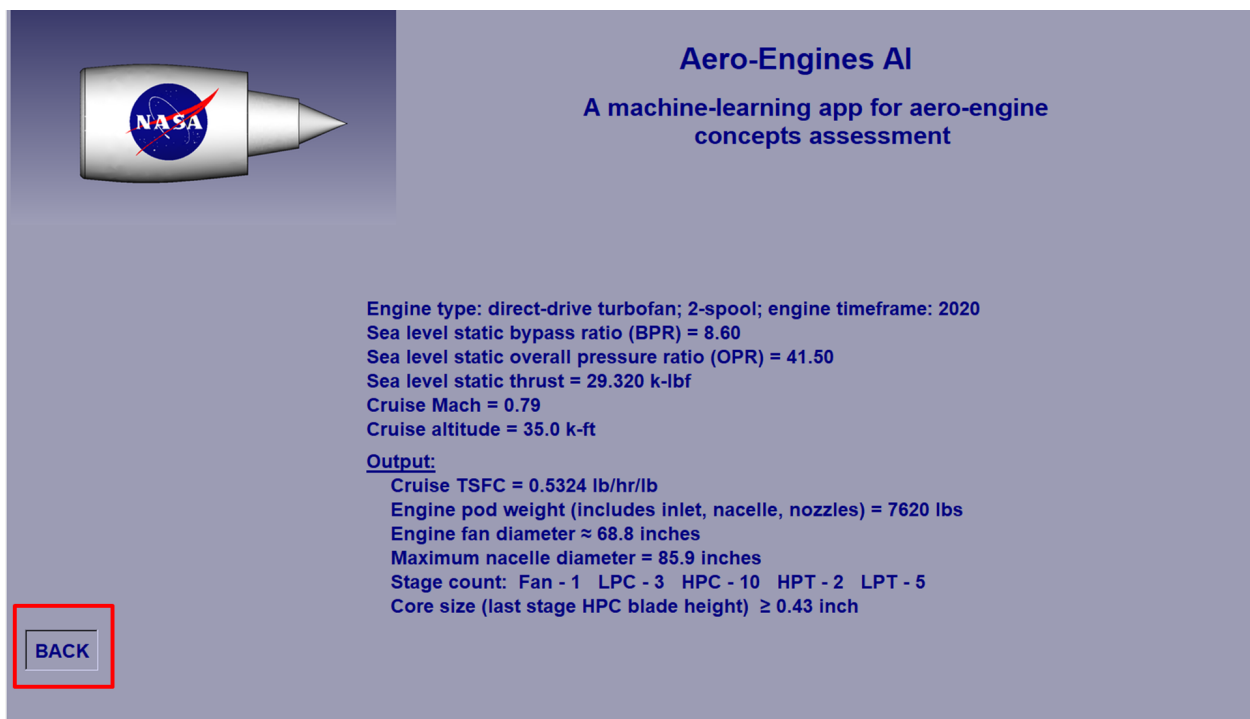
Sea level static thrust range (lbf): (min) (max) (max. no. of step)

Cruise Mach No. ($0.7 \leq M \leq 0.9$):

Cruise altitude (feet, $30000 \leq \text{alt} \leq 45000$):

PREDICT

Figure 8.—Input page for multiple-engine designs.



Aero-Engines AI
A machine-learning app for aero-engine concepts assessment

Engine type: direct-drive turbofan; 2-spool; engine timeframe: 2020
Sea level static bypass ratio (BPR) = 8.60
Sea level static overall pressure ratio (OPR) = 41.50
Sea level static thrust = 29.320 k-lbf
Cruise Mach = 0.79
Cruise altitude = 35.0 k-ft

Output:
Cruise TSFC = 0.5324 lb/hr/lb
Engine pod weight (includes inlet, nacelle, nozzles) = 7620 lbs
Engine fan diameter \approx 68.8 inches
Maximum nacelle diameter = 85.9 inches
Stage count: Fan - 1 LPC - 3 HPC - 10 HPT - 2 LPT - 5
Core size (last stage HPC blade height) \geq 0.43 inch

BACK

Figure 9.—Example output of a single-engine design.

A	B	C	D	E	F	G	H	I	J	K	L	M	N	O	P	Q	R	S
	SLS BPR	SLS Thrust, k.lbf/s	Cruise Mach	Cruise Alt, k.ft	Drive Type	No. Spool	Engine Timeframe	Fan dia, inch	Cruise TSFC, lb/hp/hr	Pod Weight, lbs	HPC last-stg blade-ht, inch	# fan stage	# LPC stage	# HPC stage	# HPT stage	# IPT stage	# LPT stage	
1	SLS OPR	26	0.8	43	geared	2-spool	2035	71.40	0.5374	6631	>0.43 inch	1	3	9	2			
2	36	11	27	43	geared	2-spool	2035	72.70	0.5418	6859	>0.43 inch	1	3	9	2			
3	36	11	28	43	geared	2-spool	2035	74.30	0.5442	7118	>0.43 inch	1	3	9	2			
4	36	11	28	43	geared	2-spool	2035	74.30	0.5442	7118	>0.43 inch	1	3	9	2			
5	36	12	26	43	geared	2-spool	2035	73.10	0.5320	6760	>0.43 inch	1	3	9	2			
6	36	12	27	43	geared	2-spool	2035	74.60	0.5364	7020	>0.43 inch	1	3	9	2			
7	36	12	28	43	geared	2-spool	2035	76.20	0.5400	7309	>0.43 inch	1	3	9	2			
8	36	13	26	43	geared	2-spool	2035	74.80	0.5272	6907	>0.43 inch	1	3	9	2			
9	36	13	27	43	geared	2-spool	2035	76.50	0.5317	7202	>0.43 inch	1	3	9	2			
10	36	13	28	43	geared	2-spool	2035	78.40	0.5356	7500	>0.43 inch	1	3	9	2			
11	36	14	26	43	geared	2-spool	2035	75.30	0.5231	6874	>0.43 inch	1	3	9	2			
12	36	14	27	43	geared	2-spool	2035	76.90	0.5273	7160	>0.43 inch	1	3	9	2			
13	36	14	28	43	geared	2-spool	2035	78.60	0.5313	7451	>0.43 inch	1	3	9	2			
14	36	15	26	43	geared	2-spool	2035	76.60	0.5195	6947	>0.43 inch	1	4	9	2			
15	36	15	27	43	geared	2-spool	2035	78.30	0.5235	7234	>0.43 inch	1	4	9	2			
16	36	15	28	43	geared	2-spool	2035	80.00	0.5275	7529	>0.43 inch	1	4	9	2			
17	37	11	26	43	geared	2-spool	2035	71.40	0.5375	6640	>0.43 inch	1	3	9	2			
18	37	11	27	43	geared	2-spool	2035	73.00	0.5417	6863	>0.43 inch	1	3	9	2			
19	37	11	28	43	geared	2-spool	2035	74.30	0.5454	7102	>0.43 inch	1	3	9	2			
20	37	12	26	43	geared	2-spool	2035	73.50	0.5322	6795	>0.43 inch	1	3	9	2			
21	37	12	27	43	geared	2-spool	2035	74.90	0.5363	7051	>0.43 inch	1	3	9	2			
22	37	12	28	43	geared	2-spool	2035	76.50	0.5384	7317	>0.43 inch	1	3	9	2			
23	37	13	26	43	geared	2-spool	2035	75.50	0.5275	7035	>0.43 inch	1	3	9	2			
24	37	13	27	43	geared	2-spool	2035	77.60	0.5317	7327	>0.43 inch	1	3	9	2			
25	37	13	28	43	geared	2-spool	2035	79.20	0.5346	7588	>0.43 inch	1	3	9	2			
26	37	14	26	43	geared	2-spool	2035	76.00	0.5233	6950	>0.43 inch	1	4	9	2			
27	37	14	27	43	geared	2-spool	2035	77.60	0.5275	7238	>0.43 inch	1	4	9	2			
28	37	14	28	43	geared	2-spool	2035	79.40	0.5311	7525	>0.43 inch	1	4	9	2			
29	37	15	26	43	geared	2-spool	2035	76.90	0.5197	6962	>0.43 inch	1	4	9	2			
30	37	15	27	43	geared	2-spool	2035	78.50	0.5236	7246	>0.43 inch	1	4	9	2			
31	37	15	28	43	geared	2-spool	2035	80.20	0.5274	7530	>0.43 inch	1	4	9	2			
32	38	11	26	43	geared	2-spool	2035	71.50	0.5372	6658	>0.43 inch	1	3	9	2			
33	38	11	27	43	geared	2-spool	2035	73.00	0.5398	6874	>0.43 inch	1	3	9	2			
34	38	11	28	43	geared	2-spool	2035	74.40	0.5403	7112	>0.43 inch	1	3	9	2			
35	38	12	26	43	geared	2-spool	2035	73.70	0.5324	6828	>0.43 inch	1	3	9	2			
36	38	12	27	43	geared	2-spool	2035	75.20	0.5358	7079	>0.43 inch	1	3	9	2			
37	38	12	28	43	geared	2-spool	2035	76.80	0.5363	7358	>0.43 inch	1	3	9	2			
38	38	13	26	43	geared	2-spool	2035	76.40	0.5278	7088	>0.43 inch	1	4	9	2			
39	38	13	27	43	geared	2-spool	2035	78.00	0.5317	7358	>0.43 inch	1	4	9	2			
40	38	13	28	43	geared	2-spool	2035	79.50	0.5325	7601	>0.43 inch	1	4	9	2			
41	38	14	26	43	geared	2-spool	2035	77.00	0.5236	7063	>0.43 inch	1	4	9	2			
42	38	14	27	43	geared	2-spool	2035	78.70	0.5275	7359	>0.43 inch	1	4	9	2			
43	38	14	28	43	geared	2-spool	2035	80.40	0.5289	7629	>0.43 inch	1	4	9	2			
44	38	15	26	43	geared	2-spool	2035	77.60	0.5198	7045	>0.43 inch	1	4	9	2			
45	38	15	27	43	geared	2-spool	2035	79.30	0.5237	7332	>0.43 inch	1	4	9	2			
46	38	15	28	43	geared	2-spool	2035	80.90	0.5256	7598	>0.43 inch	1	4	9	2			
47																		

Figure 10.—Example spreadsheet output of multiple-engine designs.

Summary

Aero-Engines AI, a user-friendly Windows app, has been created using *tkinter*, a GUI module that is built into the standard Python library. This app is designed to deploy trained ML models to assess various aircraft engine concepts. These ML models were trained, cross-validated, and tested in Keras, an open-source neural networks API written in Python, with TensorFlow serving as the backend engine. The assessment results are presented in terms of engine TSFC, weight, core size, and turbomachinery stage counts. The seamless deployment of these ML models through the app demonstrates that *Aero-Engines AI* is an efficient and easy-to-use tool for exploring the

design space of aircraft engines during the conceptual design stage. The current version of the app focuses on predicting the performance of conventional turbofans. However, the app's scope can be easily expanded to include other engine types (such as turboshaft and hybrid-electric systems), after ML models are developed for them.

The success of the ML application will depend on the quality and quantity of data available for training, as well as the deployment of the ML model itself. Careful consideration of these factors is crucial to ensure the optimal performance of the ML system. Overall, the use of a machine-learning app for aircraft engine concept assessment represents a promising area of development in aircraft engine conceptual design.

Appendix A.—Engine Database

<u>Org.</u>	<u>Engine Model</u>	<u>BPR (SLS)</u>	<u>OPR (SLS)</u>	<u>Thrust, lbs (SLS)</u>	<u>Cruise Mach</u>	<u>Cruise Alt. k ft.</u>	<u>Year certified</u>	<u>System Type</u>	<u>No. of Spools</u>	<u>Cruise TSFC lb/lbf.hr</u>	<u>Propulsion System Weight, lbs</u>
CFM Int'l	CFM56-2C1	6.0	23.50	22000	0.80	35	1979	DD	2	0.651	7199
CFM Int'l	CFM56-3B1	5.1	22.40	20000	0.80	35	1984	DD	2	0.655	6389
CFM Int'l	CFM56-3B2	5.1	24.30	22000	0.80	35	1984	DD	2	0.655	6607
CFM Int'l	CFM56-3C1	5.1	25.50	23500	0.80	35	1986	DD	2	0.667	6766
CFM Int'l	CFM56-5A1	6.0	26.60	25000	0.80	35	1987	DD	2	0.596	7770
CFM Int'l	CFM56-5A3	6.0	27.90	26500	0.80	35	1990	DD	2	0.596	7850
CFM Int'l	CFM56-5A4	6.0	23.80	22000	0.80	35	1996	DD	2	0.596	7375
CFM Int'l	CFM56-5A5	6.0	25.10	23500	0.80	35	1996	DD	2	0.596	7534
CFM Int'l	CFM56-5B1	5.7	30.20	30000	0.80	35	1994	DD	2	0.600	8366
CFM Int'l	CFM56-5B2	5.6	31.30	31000	0.80	35	1993	DD	2	0.600	8479
CFM Int'l	CFM56-5B3	5.4	32.60	33300	0.80	35	1997	DD	2	0.600	8734
CFM Int'l	CFM56-5B4	5.9	27.10	27000	0.80	35	1994	DD	2	0.600	8036
CFM Int'l	CFM56-5B5/P	5.9	23.33	22000	0.80	35	1996	DD	2	0.600	7509
CFM Int'l	CFM56-5B6/P	6.0	24.64	23500	0.80	35	1995	DD	2	0.600	7659
CFM Int'l	CFM56-5C2	6.8	28.80	31200	0.80	35	1991	DD	2	0.545	8796
CFM Int'l	CFM56-5C3	6.7	29.90	32500	0.80	35	1994	DD	2	0.567	9122
CFM Int'l	CFM56-5C4	6.6	31.15	34000	0.80	35	1994	DD	2	0.567	9285
CFM Int'l	CFM56-7B20	5.4	22.61	20600	0.80	35	1996	DD	2	0.603	6963
CFM Int'l	CFM56-7B22	5.3	24.41	22700	0.80	35	1996	DD	2	0.603	7194
CFM Int'l	CFM56-7B24	5.2	25.78	24200	0.80	35	1996	DD	2	0.603	7360
CFM Int'l	CFM56-7B26	5.1	27.61	26300	0.80	35	1996	DD	2	0.603	7602
CFM Int'l	CFM56-7B27	5.0	28.63	27300	0.80	35	1996	DD	2	0.603	7872
CFM Int'l	LEAP-1A26	11.1	33.40	27112	0.78	35	2015	DD	2	0.536	8840
CFM Int'l	LEAP-1A35	10.7	38.60	32170	0.78	35	2015	DD	2	0.536	9401
CFM Int'l	LEAP-1B25	8.4	38.40	26797	0.79	35	2016	DD	2	0.536	7778
CFM Int'l	LEAP-1B27	8.5	39.90	28034	0.79	35	2016	DD	2	0.536	7898
CFM Int'l	LEAP-1B28	8.6	41.50	29315	0.79	35	2016	DD	2	0.536	8024
GE	CF6-6D	5.9	24.70	40000	0.85	35	1970	DD	2	0.646	11749
GE	CF6-6D1	5.9	24.70	41500	0.85	35	1971	DD	2	0.646	11895
GE	CF6-6D1A	5.9	25.40	41500	0.85	35	1971	DD	2	0.646	11895
GE	CF6-45A2	4.3	25.90	46500	0.85	35	1973	DD	2	0.630	12927
GE	CF6-50C	4.3	28.80	51000	0.85	35	1975	DD	2	0.657	13323
GE	CF6-50C1	4.3	29.80	52500	0.85	35	1975	DD	2	0.657	13467
GE	CF6-50C2	4.3	28.44	52500	0.85	35	1978	DD	2	0.630	13467
GE	CF6-50C2B	4.3	29.06	54000	0.85	35	1979	DD	2	0.630	13611
GE	CF6-50E	4.3	28.44	52500	0.85	35	1973	DD	2	0.657	13505
GE	CF6-50E2	4.3	29.80	52500	0.85	35	1973	DD	2	0.630	13505
GE	CF6-80A	5.0	29.00	48000	0.80	35	1981	DD	2	0.623	12883
GE	CF6-80A2	5.0	30.10	50000	0.80	35	1981	DD	2	0.623	13076
GE	CF6-80A3	5.0	30.10	50000	0.80	35	1981	DD	2	0.623	13069
GE	CF6-80C2A1	5.1	30.96	59000	0.80	35	1985	DD	2	0.576	14782
GE	CF6-80C2A2	5.1	28.00	52460	0.80	35	1986	DD	2	0.578	14034
GE	CF6-80C2A3	5.1	31.64	58950	0.80	35	1988	DD	2	0.576	14776
GE	CF6-80C2A5	5.1	31.58	60100	0.80	35	1988	DD	2	0.578	14907
GE	CF6-80C2A8	5.1	31.00	59000	0.80	35	1996	DD	2	0.602	14782
GE	CF6-80C2B1	5.1	30.08	56700	0.80	35	1987	DD	2	0.576	14529
GE	CF6-80C2B1F	5.1	30.13	57160	0.80	35	1989	DD	2	0.564	14628
GE	CF6-80C2B2	5.1	27.74	51590	0.80	35	1987	DD	2	0.576	14039
GE	CF6-80C2B4	5.1	30.36	57180	0.80	35	1987	DD	2	0.590	14575
GE	CF6-80C2B6	5.1	31.56	60070	0.80	35	1987	DD	2	0.602	14851
GE	CF6-80E1A1	5.1	32.46	67500	0.80	35	1993	DD	2	0.562	14844
GE	CF6-80E1A2	5.1	33.10	68240	0.80	35	1993	DD	2	0.562	14844
GE	CF6-80E1A3	5.1	35.70	68520	0.80	35	2001	DD	2	0.562	14844
GE	CF6-80E1A4	5.1	34.50	66870	0.80	35	1997	DD	2	0.562	14844
GE	CF34-10A	5.4	26.50	18290	0.74	37	2010	DD	2	0.650	5453
GE	CF34-10E	5.1	27.30	18820	0.74	37	2002	DD	2	0.665	5598
GE	CF34-3A	6.3	19.70	9220	0.74	37	1986	DD	2	0.704	2849
GE	CF34-8C1	5.1	23.03	12670	0.74	37	1999	DD	2	0.664	3988
GE	CF34-8C5	5.1	23.09	13358	0.74	37	2002	DD	2	0.680	3935
GE	CF34-8E5A2	5.1	24.82	14500	0.74	37	2002	DD	2	0.680	4129
GE	GE90-76B	8.6	35.45	79654	0.80	35	1995	DD	2	0.545	20930

System type: DD = direct-drive system
G = geared system

Appendix A.—Continued

Org.	Engine Model	Thrust, lbs			Cruise	Cruise Alt.	Year	System	No. of	Cruise TSFC	Propulsion System
		BPR (SLS)	OPR (SLS)	(SLS)	Mach	k ft.	certified	Type	Spools	lb/lbf.hr	Weight, lbs
GE	GE90-85B	8.4	38.37	87315	0.80	35	1995	DD	2	0.553	21656
GE	GE90-90B	8.4	39.70	94000	0.80	35	1997	DD	2	0.545	22280
GE	GE90-94B	8.3	40.53	97300	0.80	35	2000	DD	2	0.545	22592
GE	GE90-115B	7.1	42.24	115529	0.80	35	2003	DD	2	0.550	25876
GE	GEnx-1B54	9.4	35.20	57394	0.85	40	2008	DD	2	0.514	16594
GE	GEnx-1B58	9.2	37.20	60991	0.85	40	2008	DD	2	0.514	16952
GE	GEnx-1B64	9.0	40.60	66993	0.85	40	2008	DD	2	0.514	17537
GE	GEnx-1B70	8.8	43.50	72299	0.85	40	2008	DD	2	0.514	18054
P&W	JT8D-7	1.1	15.82	14000	0.80	35	1966	DD	2	0.796	4508
P&W	JT8D-9	1.0	15.88	14500	0.80	35	1967	DD	2	0.807	4646
P&W	JT8D-17AR	1.0	17.28	16400	0.80	35	1982	DD	2	0.825	4910
P&W	JT8D-17R	1.0	18.24	17400	0.80	35	1976	DD	2	0.825	5009
P&W	JT8D-209	1.8	18.30	18500	0.80	35	1979	DD	2	0.724	5905
P&W	JT8D-219	1.7	20.27	21000	0.80	35	1985	DD	2	0.737	6266
P&W	JT9D-3A	5.2	21.50	44300	0.85	35	1969	DD	2	0.624	12794
P&W	JT9D-7	5.2	22.20	46300	0.85	35	1971	DD	2	0.620	13102
P&W	JT9D-7A	5.1	20.30	46950	0.85	35	1972	DD	2	0.625	13169
P&W	JT9D-7F	5.1	22.80	48000	0.85	35	1974	DD	2	0.631	13270
P&W	JT9D-7J	5.1	23.50	50000	0.85	35	1976	DD	2	0.631	13468
P&W	JT9D-7Q	4.9	24.50	53000	0.85	35	1978	DD	2	0.631	14055
P&W	JT9D-7R4D	5.0	23.40	48000	0.85	35	1978	DD	2	0.615	13553
P&W	JT9D-7R4E	5.0	24.20	50000	0.85	35	1982	DD	2	0.620	13565
P&W	JT9D-7R4G2	4.8	26.30	54750	0.85	35	1982	DD	2	0.639	14220
P&W	JT9D-7R4H1	4.8	26.70	56000	0.85	35	1982	DD	2	0.628	14340
P&W	JT9D-20	5.2	20.30	46300	0.85	35	1972	DD	2	0.624	13097
P&W	JT9D-70A	4.9	24.50	53000	0.85	35	1974	DD	2	0.631	13990
P&W	1127G	12.3	31.70	27000	0.78	35	2014	G	2	0.530	6300
P&W	1519G	11.6	32.30	19000	0.78	35	2013	G	2	0.544	4800
P&W	2037	6.0	26.90	37600	0.80	35	1983	DD	2	0.563	10607
P&W	2040	5.5	29.40	40900	0.80	35	1987	DD	2	0.563	10972
P&W	2043	5.3	31.90	42600	0.80	35	1995	DD	2	0.563	11159
P&W	4052	5.0	26.32	52200	0.85	35	1987	DD	2	0.560	14027
P&W	4056	4.7	29.30	56750	0.85	35	1986	DD	2	0.560	14490
P&W	4060	4.5	32.40	60000	0.85	35	1988	DD	2	0.560	14819
P&W	4074	6.8	32.20	74500	0.85	35	1994	DD	2	0.560	19457
P&W	4077	6.7	33.20	77000	0.85	35	1994	DD	2	0.560	19950
P&W	4084	6.4	36.20	84000	0.85	35	1994	DD	2	0.560	20549
P&W	4090	6.1	39.16	90200	0.85	35	1996	DD	2	0.560	21522
P&W	4098	5.8	41.37	95340	0.85	35	1998	DD	2	0.560	22025
P&W	4152	4.9	26.90	52200	0.85	35	1986	DD	2	0.560	14036
P&W	4156	4.7	29.30	56750	0.85	35	1986	DD	2	0.560	14490
P&W	4164	5.2	31.24	64000	0.85	35	1993	DD	2	0.560	16886
P&W	4168-1D	4.9	33.10	68600	0.85	35	2008	DD	2	0.560	17345
P&W	4460	4.7	30.68	60000	0.85	35	1988	DD	2	0.560	14802
P&W	4462	4.6	31.91	63300	0.85	35	1992	DD	2	0.560	15126
P&W	6122A	4.8	25.70	22100	0.80	35	2004	DD	2	0.540	6311
Rolls-Royce	RB211-22B	4.7	25.00	41000	0.85	35	1973	DD	3	0.655	12098
Rolls-Royce	RB211-524B	4.5	28.40	49100	0.85	35	1973	DD	3	0.633	13270
Rolls-Royce	RB211-524B4-02	4.4	29.00	50000	0.85	35	1981	DD	3	0.603	13309
Rolls-Royce	RB211-524C2	4.5	29.10	51500	0.85	35	1979	DD	3	0.656	13370
Rolls-Royce	RB211-524D4	4.3	29.70	53000	0.85	35	1983	DD	3	0.631	13606
Rolls-Royce	RB211-524G	4.3	32.10	58000	0.85	35	1989	DD	3	0.582	14040
Rolls-Royce	RB211-524H	4.2	34.00	60600	0.85	35	1989	DD	3	0.572	14186
Rolls-Royce	RB211-535C	4.5	21.50	37400	0.80	35	1981	DD	3	0.646	10338
Rolls-Royce	RB211-535E4	4.1	25.40	40100	0.80	35	1983	DD	3	0.598	10648
Rolls-Royce	AE3007A	5.2	18.08	7580	0.78	32	1997	DD	2	0.625	2332
Rolls-Royce	BR710-A1-10	4.2	24.23	14750	0.80	35	1996	DD	2	0.630	4640
Rolls-Royce	BR715-A1-30	4.7	28.98	18920	0.76	35	1998	DD	2	0.620	6155
Rolls-Royce	BR715-C1-30	4.6	32.15	21430	0.76	35	1998	DD	2	0.620	6155
Rolls-Royce	Trent 1000-A	9.5	41.00	70000	0.85	35	2007	DD	3	0.506	18056
Rolls-Royce	Trent 553-61	7.5	35.19	56620	0.82	35	2000	DD	3	0.539	14843

System type: DD = direct-drive system
G = geared system

Appendix A.—Concluded

Org.	Engine Model	Thrust, lbs			Cruise	Cruise Alt.	Year	System	No. of	Cruise TSFC	Propulsion System
		BPR (SLS)	OPR (SLS)	(SLS)	Mach	k ft.	certified	Type	Spools	lb/lbf.hr	Weight, lbs
Rolls-Royce	Trent 556-61	7.5	36.70	56620	0.82	35	2000	DD	3	0.539	14843
Rolls-Royce	Trent 7000-72	9.0	45.40	73700	0.85	35	2018	DD	3	0.506	18864
Rolls-Royce	Trent 768	5.2	34.00	68400	0.82	35	1994	DD	3	0.565	16839
Rolls-Royce	Trent 772	5.0	35.80	71100	0.82	35	1994	DD	3	0.565	17105
Rolls-Royce	Trent 772B-60	4.9	36.80	72000	0.82	35	1998	DD	3	0.565	17215
Rolls-Royce	Trent 875	6.1	35.42	79100	0.83	35	1995	DD	3	0.560	19430
Rolls-Royce	Trent 877	6.0	36.30	81300	0.83	35	1995	DD	3	0.560	19650
Rolls-Royce	Trent 884	5.9	38.96	87700	0.83	35	1995	DD	3	0.560	20284
Rolls-Royce	Trent 890-17	6.2	40.70	91300	0.83	35	1995	DD	3	0.560	20602
Rolls-Royce	Trent 892	5.7	41.38	92500	0.83	35	1997	DD	3	0.560	20762
Rolls-Royce	Trent 895	5.7	41.52	92900	0.83	35	1999	DD	3	0.560	20801
Rolls-Royce	Trent 970-84	8.5	38.00	76100	0.85	35	2006	DD	3	0.518	19379
Rolls-Royce	Trent XWB-84	9.0	41.10	85200	0.85	35	2013	DD	3	0.488	21163
Rolls-Royce	Trent XWB-97	8.0	48.60	98200	0.85	35	2017	DD	3	0.488	22771
IAE	V2500-A1	5.3	29.80	25000	0.80	35	1988	DD	2	0.580	7300
IAE	V2522-A5	4.9	25.70	23043	0.80	35	1996	DD	2	0.575	7500
IAE	V2524-A5	4.8	26.90	24518	0.80	35	1996	DD	2	0.575	7597
IAE	V2525-D5	4.8	27.20	25000	0.80	35	1992	DD	2	0.575	7900
IAE	V2527-A5	4.8	27.20	25000	0.80	35	1992	DD	2	0.575	7651
IAE	V2528-D5	4.7	30.00	28000	0.80	35	1992	DD	2	0.575	8140
IAE	V2530-A5	4.6	32.00	29900	0.80	35	1992	DD	2	0.575	8219
IAE	V2533-A5	4.5	33.44	31600	0.80	35	1996	DD	2	0.575	8420
NASA SFW	UHB	18.8	44.7	36833	0.80	35	2015	G	2	0.477	9300
NASA AATT	N3CC-2016	17.6	31.6	18830	0.70	35	2040	G	2	0.461	5343
NASA AATT	N3CC-2017	17.3	36.9	21515	0.78	35	2040	G	2	0.485	6012
NASA AATT	N+3	27.5	36.6	28620	0.80	35	2040	G	2	0.464	9354
NASA AATT	Small Core geared	25.5	38.8	37659	0.80	35	2040	G	2	0.460	12152
NASA AATT	N3CC-2018	21.6	36.7	21662	0.79	37.7	2040	G	2	0.479	6007
NASA ERA	Large-DD-2015	16.6	43.7	71792	0.80	35	2030	DD	2	0.480	21399
NASA ERA	Large-DD-2015-HWB-V1	14.4	48.9	67183	0.80	35	2030	DD	2	0.485	18768
NASA ERA	Large-DD-2015-HWB-V2	13.7	49.8	67233	0.80	35	2030	DD	2	0.487	18832
NASA ERA	Large-Geared-2015-HWB-V3	20.0	47.2	56172	0.80	35	2030	G	2	0.465	15591
NASA ERA	Large-Geared-2015-HWB-V2	20.0	47.1	67423	0.80	35	2030	G	2	0.464	18823
NASA ERA	Large-Geared-2015-HWB	19.3	47.2	67386	0.80	35	2030	G	2	0.466	18823
NASA ERA	Large-Geared-2015	24.7	39.9	74149	0.80	35	2030	G	2	0.458	23023
NASA ERA	Medium-Geared-2015	23.9	38.4	45829	0.80	35	2030	G	2	0.466	13631
NASA ERA	Medium-Geared-2015-V2	24.8	38.5	45799	0.80	35	2030	G	2	0.465	13668
NASA ERA	Small-DD-2015	9.9	28.7	14647	0.80	35	2030	DD	2	0.526	3815
NASA ERA	Small-DD-2015-V2	10.0	28.7	14686	0.80	35	2030	DD	2	0.525	3812
NASA ERA	Small-Geared-2015	27.0	24.6	21525	0.80	35	2030	G	2	0.485	6203
NASA ERA	Small-Geared-2015-V2	27.4	24.8	21553	0.80	35	2030	G	2	0.483	6232
NASA ERA	Large-DD-2014	16.2	47.4	80071	0.80	35	2030	DD	2	0.469	22534
NASA ERA	Large-Geared-2014	22.4	47.2	87496	0.80	35	2030	G	2	0.458	23248
NASA ERA	Medium-Geared-2014	22.4	44.7	51295	0.80	35	2030	G	2	0.467	12645
NASA ERA	Small-DD-2014	9.8	29.7	15566	0.80	35	2030	DD	2	0.519	3833
NASA ERA	Small-Geared-2014	24.7	29.2	24887	0.80	35	2030	G	2	0.486	5913
NASA SFW	SA-FPR1.4-DD-2D	18.4	33.1	23813	0.80	35	2025	DD	2	0.479	10563
NASA SFW	SA-FPR1.5-DD-2D	15.0	33.8	23370	0.80	35	2025	DD	2	0.496	7965
NASA SFW	SA-FPR1.6-DD-2D	12.7	34.4	23046	0.80	35	2025	DD	2	0.510	6592
NASA SFW	SA-FPR1.7-DD-2D	10.9	35	22734	0.80	35	2025	DD	2	0.525	6099
NASA SFW	SA-FPR1.3-GR-HW-2D	24.1	32.6	26343	0.80	35	2025	G	2	0.470	8736
NASA SFW	SA-FPR1.4-GR-HW-2D	17.5	33.8	24917	0.80	35	2025	G	2	0.486	7401
NASA SFW	SA-FPR1.5-GR-HW-2D	14.6	33.5	23369	0.80	35	2025	G	2	0.502	6626
NASA SFW	SA-FPR1.6-GR-HW-2D	12.4	34	22924	0.80	35	2025	G	2	0.517	6252
NASA SFW	SA-FPR1.3-GR-HW-2E	26.0	32.3	28358	0.80	35	2025	G	2	0.473	8550
NASA SFW	SA-FPR1.4-GR-HW-2E	18.0	33.8	26575	0.80	35	2025	G	2	0.495	7123
NASA SFW	SA-FPR1.5-GR-HW-2E	12.1	35.4	24686	0.80	35	2025	G	2	0.515	6305
NASA SFW	SA-FPR1.6-GR-HW-2E	9.9	36.3	24262	0.80	35	2025	G	2	0.534	5896
NASA SFW	SA-FPR1.7-DD-LW-2E	8.5	37.6	23889	0.80	35	2025	DD	2	0.547	5561
NASA SFW	Simulated Genx	9.2	41.4	63800	0.85	35	2008	DD	2	0.523	17198
NASA SFW	Simulated GE90-110B	7.2	42	110000	0.85	35	2003	DD	2	0.549	23728

System type: DD = direct-drive system
G = geared system

SFW—Subsonic Fixed Wing project
ERA—Environmentally Responsible Aviation project
AATT—Advanced Air Transport Technology project

References

1. Tong, M. T., "Using Machine Learning to Predict Core Sizes of High-Efficiency Turbofan Engines," GTP-19-1338, ASME Journal of Engineering for Gas Turbines and Power, Volume 141, Issue 11, November 2019.
2. Tong, M. T., "Machine Learning-Based Predictive Analytics for Aircraft Engine Conceptual Design," NASA TM-20205007448, October 2020.
3. Tong, M. T., "A Machine-Learning Approach to Assess Aircraft Engine System Performance," GT-2020-14661, Proceedings of ASME Turbo Expo 2020, September 21–25, 2020 (virtual conference).
4. Daly, M., 2018, "Jane's Aero-Engine," IHS, London, UK.
5. Meier, N., 2018, "Civil Turbojet/Turbofan Specifications," accessed Aug. 8, 2018, <http://www.jet-engine.net/civtfspec.html>
6. GE Aviation, 2018, "GE Aviation," GE Aviation, Evendale, OH, accessed Aug. 8, 2018, <https://www.geaviation.com/commercial>
7. Pratt and Whitney, 2018, "Commercial-Engines," Pratt and Whitney, East Hartford, CT, accessed Aug. 8, 2018, <https://www.pw.utc.com/products-and-services/products/commercial-engines>
8. Rolls Royce, 2018, "Rolls Royce," Rolls Royce, Derby, UK, accessed Aug. 8, 2018, <https://www.rolls-royce.com/products-and-services/civil-aerospace>
9. CFM International, 2018, "CFM International," CFM International, Cincinnati, OH, accessed Aug. 8, 2018, <https://www.cfmaeroengines.com/>
10. International Civil Aviation Organization, 2018, "ICAO Aircraft Emissions Databank," International Civil Aviation Organization, Montreal, Canada.
11. Guynn, M.D., Berton, J.J., Fisher, K.L., Haller, W.J., Tong, M., Thurman, D.R., "Engine Conceptual Study for an Advanced Single-Aisle Transport," NASA TM-2009-215784, August 2009.
12. Guynn, M.D., Berton, J.J., Fisher, K.L., Haller, W.J., Tong, M., Thurman, D.R., "Analysis of Turbofan Design Options for an Advanced Single-Aisle Transport Aircraft," AIAA 2009-6942, September 2009.
13. Guynn, M. D., Berton, J.J., Fisher, K.L., Haller, W.J., Tong, M., Thurman, D.R., "Refined Exploration of Turbofan Design Options for an Advanced Single-Aisle Transport," NASA TM-2011-216883, January 2011.
14. Guynn, M.D., Berton, J.J., Tong, M.T., Haller, W.J., "Advanced Single-Aisle Transport Propulsion Design Options Revisited," AIAA 2013-4330, August 2013.
15. Nickol, C.L. and Haller W.J., "Assessment of the Performance Potential of Advanced Subsonic Transport Concepts for NASA's Environmentally Responsible Aviation Project," AIAA 2016-1030, January 2016.
16. Collier, F., Thomas, R., Burley, C., Nickol, C., Lee, C.M., Tong, M., "Environmentally Responsible Aviation – Real Solutions for Environmental Challenges Facing Aviation," 27th International Congress of the Aeronautical Sciences, September, 2010.
17. Geron, A., "Hands-On Machine Learning with Scikit-Learn and TensorFlow," first edition, March 2017. Published by O'Reilly Media, Inc.
18. Chollet, François and others, "Keras." accessed February 22, 2019, <https://keras.io/>
19. Google, "TensorFlow: Large-Scale Machine Learning on Heterogeneous Distributed Systems." accessed February 20, 2019, <https://www.tensorflow.org/>
20. Ng, A., 2004 "Feature selection, L_1 vs. L_2 regularization, and rotational invariance," Proceedings of the twenty-first international conference on Machine learning, July 4, 2004
21. Hinton, G.E., Krizhevsky, A., Srivastava, N., Sutskever, I., & Salakhutdinov, R., "Dropout: A simple Way to Prevent Neural Networks from Overfitting." Journal of Machine Learning Research, 15, 1929-1958. June, 2014.
22. Kingma, D. P. and Ba, J., "Adam: A Method for Stochastic Optimization," International Conference on Learning Representations, May 2015.
23. Van Rossum, G., et al., "The Python Library Reference, release 3.8.2," Python Software Foundation, 2020.
24. Cortesi, D., "PyInstaller 5.7.0," released on December 4, 2022, accessed December 19, 2022. <https://pypi.org/project/pyinstaller/>

